

Transformations and Microstructures

Present status of and future prospects for precipitation research in the steel industry (Review)

T.SENUMA

Precipitation is one of the most important phenomena for controlling the properties of steel. Therefore, numerous studies have been performed in this field. Since 1998, the ISIJ has held a research workshop on precipitation control consisting of around forty members from academia and industry. This workshop held a seminar in autumn 2001 in which some of the workshop members, most of whom were from academia will surveyed the present status of precipitation research from an academic viewpoint. In this connection, a review of the present status and future prospects of precipitation research in the steel industry was requested so that an understanding as to how precipitation control was applied in practice could be obtained.

This paper is a modified English version of said Japanese review and the recent industrial research on the precipitation control in steel sheets is reviewed and the resultant new products are introduced.

(cf. *ISIJ Int.*, 42 (2002), 1)

Fundamentals of High Temperature Processes

Intensive improvement of reduction rate of hematite-graphite mixture by mechanical milling

J.Y.KHAKI *et al.*

The effect of ball milling of raw materials on the reaction behavior of composite mixture of hematite and graphite have been studied. Hematite was mixed with 19.84 wt% graphite (C/O ratio was 1.1 in composite mixture) and subjected to ball milling. The milling time was changed from 6 to 100 hr with the hematite-graphite mixture. On the other hand, graphite or hematite was milled alone and then mixed with non-milled hematite or graphite, respectively. The effect of milling time on reduction process in an Ar atmosphere was studied by TG-DTA. The samples were heated by a constant heating rate of 10°C/min from room temperature up to 1100°C and maintained for 30 min at this temperature.

The rate of reaction (RTG) was obtained by the differentiation of weight loss curve. It was found that the RTG curve consisted of three reaction curves which were hematite-magnetite (HM), magnetite-wüstite (MW) and wüstite-metallic iron (WF) reductions. The curve corresponding to the HM reduction located in low temperature range and stood alone from other two reduction curves (MW and WF reductions). The curves of MW and WF reductions were overlapped. The pulse-like reduction curve corresponding to WF reduction was observed in the longer milling time, which meant extremely high rate of reduction.

The temperatures decreased and the reaction degrees at each peaks increased with increasing milling time.

The kinetic analysis applying the single and consecutive reaction was carried out. The calculated

reaction curves were in good agreement with the observations which showed that the reaction mainly occurred in this system was the solid oxide-solid carbon reaction. The variation of parameters of rate constant presented the different mechanism of reaction between shorter and longer milling time at the border of 24 hr.

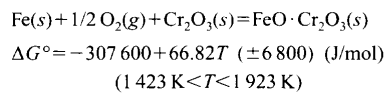
(cf. *ISIJ Int.*, 42 (2002), 13)

Thermodynamics of Oxygen in Liquid Fe-Cr Alloy Saturated with FeO·Cr₂O₃ Solid Solution

M.KIMOTO *et al.*

The equilibrium relation between dissolved Cr and O in liquid high Cr steel has been assessed on the condition of pure solid Cr₂O₃ saturation in our previous paper. Following this, the present work deals with the equilibrium between Cr and O in liquid iron saturated with FeO·Cr₂O₃ solid solution and phase equilibria among liquid Fe-Cr alloy and Cr₂O₃ containing oxides for the full understanding of the thermodynamic behavior of oxygen in liquid Fe-Cr alloy. The free energy of formation of FeO·Cr₂O₃ and activities of the constituents in FeO·Cr₂O₃ solid solution have also been measured by the chemical equilibrium technique at 1 823 to 1 923 K.

The free energy of formation of FeO·Cr₂O₃ was given by the following equation.



The activities of Fe₂O(l) and Cr₂O₃(s) in FeO·Cr₂O₃ solid solution exhibit negative deviation from ideality. The oxide phase in equilibrium with liquid Fe-Cr alloy is not Cr₂O₃ but FeO·Cr₂O₃ solid solution when Cr content in metal is less than the critical Cr content of approximately 7 mass%. The present experimental results are in good accord with the thermodynamic relation between dissolved Cr and O calculated by the parameters which have been proposed in our previous work, if appropriate correction for Cr₂O₃ activity is applied.

(cf. *ISIJ Int.*, 42 (2002), 23)

Phase equilibria between SiO₂ and iron-chromite spinel structure solid solution, and deoxidation of liquid Fe-Cr alloy with silicon

T.ITOH *et al.*

Oxygen control in liquid stainless steel production is extremely important for the removal of impurities and improvement of Cr yield. Precise information on the thermodynamics of oxygen in liquid Fe-Cr alloy is necessary for this purpose. The equilibrium relation between dissolved Cr and O in liquid iron saturated with pure solid Cr₂O₃ or FeO·Cr₂O₃ solid solution and thermodynamic behavior of FeO·Cr₂O₃ solid solution had been established in our previous works. Following these studies, the deoxidation equilibrium of Si in liquid Fe-Cr alloy was thermodynamically discussed in this paper. Mutual solubility between SiO₂ and (Fe,Mg)O·(Cr,Al)₂O₃ solid solution was observed at 1 573 and 1 873 K, in order to know the activity of SiO₂ coexisted with Cr₂O₃ based oxide solid solution after Si deoxidation of liquid Fe-Cr alloy. It was found that

Si deoxidation equilibrium of liquid Fe-Cr alloy could be thermodynamically evaluated based on unit activity of SiO₂ due to negligibly small mutual solubility between SiO₂ and FeO·Cr₂O₃ based solid solution. As the result, the deoxidation power of Si would not enough high to produce low oxygen high Cr steel because of the attraction between Cr and Si in liquid iron.

(cf. *ISIJ Int.*, 42 (2002), 33)

Structural investigation of CaO-Al₂O₃ and CaO-Al₂O₃-CaF₂ slags via fourier transform infrared spectra

J.H.PARK *et al.*

The FT-IR spectra of the CaO-Al₂O₃ and CaO-Al₂O₃-CaF₂ slags were measured to understand the structural aspects of (fluoro-) aluminate slags. The infrared spectra of the CaO-Al₂O₃ slag was interpreted based on the relationship between bond length and force constant of Al-O bond. Thereafter, the role of F⁻ ions in the depolymerization of aluminate network was discussed. The wavenumbers of [AlO₄]-tetrahedra higher than that of [AlO₆]-octahedra would be originated from the Al-O bond length in tetrahedra shorter than that in octahedra. In the CaO_{satd}-Al₂O₃-CaF₂ system, the IR-transmitting bands of [AlO_nF_{4-n}]-complexes are observed through the entire composition of the fluoroaluminate system, while the bands of [AlO₄]-tetrahedra, [AlO₆]- and [AlF₆]-octahedra appear in the composition less than 24.0 (mol%) CaF₂. In the 26.2 (mol%) Al₂O₃-containing system, the bands of interlinked [AlO₄]-tetrahedra are shown at only 2-liquids boundary, while these bands are shown in the whole composition region in the 41.5 (mol%) Al₂O₃-containing system. In the 41.7 and 51.0 (mol%) CaO-Al₂O₃-CaF₂ systems, the transmitting bands of [AlO_nF_{4-n}]-complexes are observed through the entire composition, while those of [AlO₄]-tetrahedra are shown in the composition of X_{CaF₂}/X_{Al₂O₃} ≤ 1.0. Also, the relative intensity of the bands indicating [AlO₄]-tetrahedra in the 51.0 (mol%) CaO-containing slag is much less than that in the 41.7 (mol%) CaO-containing system.}}

(cf. *ISIJ Int.*, 42 (2002), 38)

Ironmaking

Three-dimensional multiphase mathematical modeling of the blast furnace based on the multifluid model

J.A.CASTRO *et al.*

The blast furnace process is a multi-phase chemical reactor whose main purpose is to reduce iron oxides producing hot metal. In the actual blast furnace operation several phases simultaneously interact with one another exchanging momentum, mass and energy. In this paper a three-dimensional multiphase mathematical model of the blast furnace is presented. This model treats the blast furnace process as a multiphase reactor in which all phases behave like fluids. Five phases are treated by this model, namely, gas, lump solids (iron ore, sinter, pellets and coke), pig iron, molten slag and pulverized coal. Conservation equations for mass, momentum, energy and

chemical species for all phases are solved based on the finite volume method. In the discretized momentum equations, the covariant velocity projections are used, which is expected to give the best coupling between the velocity and pressure fields and improve the convergence of the calculations. This is a new feature of the present model regarding to the numerical procedures applied to the blast furnace modeling, which emphasizes its originality. In addition, gas and solid phases are treated as continuous phases possessing a pressure field and the SIMPLE algorithm is applied to extract the pressure field and ensure mass conservation. Hot metal, slag and pulverized coal are treated as discontinuous phases consisting of unconnected droplets. For such phases, momentum conservation is used to calculate the fields of velocity while the continuity equations are used to calculate the phase volume fractions.

This model was applied to predict the three-dimensional blast furnace operation and predicted temperature distributions and operational parameters like productivity, coke rate and slag rate presented close agreement with the actual measured ones in the blast furnace process.

(cf. *ISIJ Int.*, **42** (2002), 44)

Steelmaking

Numerical analysis on the similarity between steel ladles and hot-water models regarding natural convection phenomena

Y.PAN et al.

The similarity between steel ladles and hot-water models regarding natural convection phenomena has been systematically analysed through examination of the numerical solutions of turbulent Navier–Stokes partial differential equations governing the phenomena in question. The numerical solutions have been obtained by using a computational fluid dynamics (CFD) simulation method. Key similarity criteria for non-isothermal physical modelling of steel ladles with hot-water models have been derived as

$$Fr_m = Fr_p \quad \text{and} \quad (\beta\Delta T)_m = (\beta\Delta T)_p$$

where the subscripts m and p stand for the water model and the prototype steel ladle, respectively. Accordingly, appropriate conditions fulfilling the above criteria, such as model size, water temperature, time scale factor and the scale factor of boundary heat loss fluxes, have been proposed and discussed. As a result, water models with geometry scales between 1/5 and 1/3 and using hot-water of temperature higher than 45°C are appropriate for simulating natural convection phenomena in steel ladles.

(cf. *ISIJ Int.*, **42** (2002), 53)

Thermodynamic properties of manganese oxide in BOF slags

S.-M.JUNG et al.

It is necessary to understand the thermodynamic properties of MnO in steelmaking slags for the smelting reduction of Mn ore in BOF process. Studies of the manganese distribution between CaO–

SiO₂–Fe₂O–MnO slags and liquid silver in equilibrium with solid Fe in the temperature range of 1623 to 1723 K were carried out under a CO/CO₂ atmosphere.

The Fe₂O content in (32.4–36.3)%CaO–(31.6–44.0)%SiO₂–(9.9–24.1)%FeO–(0.4–2.6)%Fe₂O₃–(8.9–10.8)%MnO slags was found to have a linear relationship with oxygen partial pressure. The values of Fe³⁺/Fe²⁺ in the same slag system increase by increasing the Fe₂O content. The Mn distribution ratio between slag and metal, (%MnO)/[%Mn]_{Fe–C_{sat}}, increases with FeO content in a linear relationship over the measured FeO concentration range (6.7–24.1 mass%). The Mn distribution ratio decreases with increasing CaF₂, which is believed to have the effect of increasing the activities of MnO and FeO.

Temperature dependence of equilibrium manganese distribution at $p_{O_2} = 6.6 \times 10^{-12}$ atm in the temperature range of 1623 to 1723 K can be expressed as follows:

$$\log \frac{(\text{MnO})}{[\% \text{Mn}]_{\text{Fe-C}_{\text{sat}}}} = \frac{14270}{T} - 6.55$$

The relative partial heat of solution of MnO into (32.7–39.1)%CaO–(32.7–38.8)%SiO₂–(10.2–20.78)%FeO–(1.0–2.4)%Fe₂O₃–(9.4–10.8)%MnO slags was estimated to be 198 kJ/mol.

(cf. *ISIJ Int.*, **42** (2002), 63)

Instrumentation, Control and System Engineering

Factors on the measurement of effective thermal diffusivity of molten slag using double hot thermocouple technique

Y.KASHIWAYA et al.

The molten slags that are used not only in the continuous caster but also in every metal industry play an important role and affect the quality of products. The authors initially developed the double hot thermocouple technique (DHTT) for *in situ* observation of mold slag crystallization.

In this study, the DHTT was further developed to allow the measurement of the overall thermal diffusivity of molten slag applying the principle of the laser flash method. The affecting factors (finite pulse time, shape of pulse and heat loss from sample surface) on the measurement of thermal diffusivity using the DHTT were discussed theoretically using both the analytical and the numerical methods. New relationship between the thermal diffusivity α and the time at half-maximum temperature $t_{0.5}$ was obtained as follows:

$$\alpha (\times 10^4 \text{ m}^2/\text{s}) = 0.000707 (t_{0.5}/t_p)^{-1.8946}$$

The thermal diffusivity obtained from the experimental half-maximum time $t_{0.5}/t_p$ (t_p is the time of peak on the heat pulse) was in good agreement with the one from literature.

(cf. *ISIJ Int.*, **42** (2002), 71)

Surface Treatment and Corrosion

Effect of mg and Si on the microstructure and corrosion behavior of Zn–Al hot dip coatings on low carbon steel

J.TANAKA et al.

Coatings formed on a low carbon steel by a two step hot dipping, primarily in a Zn bath and secondarily in a Zn–6Al bath with or without 0.5 mass% Mg and 0.1 mass% Si addition. The effects of the Mg and Si addition on the surface morphologies, microstructures, and corrosion characteristics of the coatings were investigated using a scanning electron microscope, a laser scanning microscope, and an electron probe microprobe analyzer. The coating formed in the Zn–6Al bath showed flaws as pores and cracks in the outer adhered layer, while there were few flaws in the Zn–6Al–0.5Mg–0.1Si bath coating. The Zn–6Al–0.5Mg–0.1Si coating has a lamellae structure developed well in the outer adhered layer and the initially formed α -Al was finer than that of the Zn–6Al coating. Corrosion in a 5% NaCl solution commenced from the α -Al phase at a very early stage and the Zn phase corroded preferentially. The Zn–6Al–0.5Mg–0.1Si coating corroded slowly and relatively homogeneously, while the Zn–6Al coating degraded locally due to a preferential corrosion along flaws. The Zn–6Al–0.5Mg–0.1Si coating incorporates Mg and Si in the outer adhered layer and Si in the inner alloy layer, making the Zn–6Al–0.5Mg–0.1Si coating more anti-corrosive.

(cf. *ISIJ Int.*, **42** (2002), 80)

Transformations and Microstructures

Decomposition of coarse grained austenite during accelerated cooling of C–Mn steels

M.FERRY et al.

The simulation of microstructural evolution of a range of C–Mn steels following high-speed continuous casting and controlled cooling was carried out using quench dilatometry. An initial coarse-grained austenitic microstructure (as expected during casting of low carbon steel strip) was produced by a high temperature austenitising treatment followed by cooling at rates up to 600°C/s. Continuous cooling transformation (CCT) diagrams for a range of cooling schedules were constructed. It was found that both cooling rate and steel composition produces a range of final microstructures from polygonal ferrite to martensite with a concomitant range in hardness. Coarse grained austenite was found to promote the formation of degenerate pearlite and bainitic microstructures. The role of alloying additions, in combination with cooling rate is discussed in the context of microstructural development and mechanical properties of as-cast low carbon steel strip.

(cf. *ISIJ Int.*, **42** (2002), 86)

***In-situ* high-temperature X-ray diffraction on the $\gamma \rightarrow \alpha$ transformation in low-carbon steels**

A. BODIN et al.

The texture development during the phase transformation of austenite to ferrite was studied by means of *in-situ* high-temperature X-ray diffraction and compared to results obtained with conventional X-ray diffraction. The *in-situ* technique proves to be an interesting addition to the existing measurement techniques. The observed orientations of the crystallographic planes in the austenite could be related by the Bain-orientation relation to the orientation in the ferrite. The results of the *in-situ* diffraction experiments could also be related to the orientations in the orientation distribution function of the final texture of the material after the measurements. There is good quantitative correspondence between the frac-

tion transformed as determined with dilatometry and high temperature X-ray diffraction. There is qualitative agreement with the equilibrium transformation as predicted by the software package MTDa-ta[®].

(cf. *ISIJ Int.*, **42** (2002), 94)

Evolution of microstructure and texture associated with ridging in ferritic stainless steels

S. PARK et al.

The evolution of microstructure and texture in two ferritic stainless steels was investigated in order to identify the existence of grain colonies associated with ridging and their origin. Special attentions were placed upon examining how the columnar crystals with an initial [001]/ND orientation in continuously-cast slabs can affect the formation of the

grain colonies or band structures in the cold-rolled sheet specimens. The rolling and recrystallization textures at each process stage were examined by the orientation distribution function (ODF). Micro-texture measurements using an electron back-scattered diffraction (EBSD) technique were carried out on the ND, RD, and TD section, respectively. The existence of grain colonies having both {001}<110> and {112}<110> orientations at the central region of the sheets was clearly identified. These orientations were caused by both the crystal rotation toward α -fibre texture, which is stable orientation during rolling and the suppressed recrystallization. The relation between the presence of grain colonies and ridging phenomena was discussed.

(cf. *ISIJ Int.*, **42** (2002), 100)